Catadioptric Projective Geometry

CHRISTOPHER GEYER AND KOSTAS DANIILIDIS

University of Pennsylvania, GRASP Laboratory, 3401 Walnut Street, 336C, Philadelphia, PA 19104-6228, USA

cgeyer@cis.upenn.edu

kostas@cis.upenn.edu

Abstract. Catadioptric sensors are devices which utilize mirrors and lenses to form a projection onto the image plane of a camera. Central catadioptric sensors are the class of these devices having a single effective viewpoint. In this paper, we propose a unifying model for the projective geometry induced by these devices and we study its properties as well as its practical implications. We show that a central catadioptric projection is equivalent to a two-step mapping via the sphere. The second step is equivalent to a stereographic projection in the case of parabolic mirrors. Conventional lens-based perspective cameras are also central catadioptric devices with a virtual planar mirror and are, thus, covered by the unifying model. We prove that for each catadioptric projection there exists a dual catadioptric projection based on the duality between points and line images (conics). It turns out that planar and parabolic mirrors build a dual catadioptric projection pair. As a practical example we describe a procedure to estimate focal length and image center from a single view of lines in arbitrary position for a parabolic catadioptric system.

Keywords: omnidirectional vision, catadioptric systems, conic sections, duality, stereographic projection, calibration

1. Introduction

A catadioptric instrument is an optical system combining reflective (catoptric) and refractive (dioptric) elements (Hecht and Zajac, 1997). Catadioptric combinations have been extensively used in telescopes in order to focus light from the stars onto the eye of the observer. The focal properties of mirrors with a conic profile were discovered by the ancient Greek geometer Diocles (Toomer, 1976) and concave mirrors have been extensively used for light concentration for energy purposes. To enhance the illumination of a scene such concave mirrors appear also in primitive organisms like deep-sea ostracodes (Land, 1981).

Catadioptric systems have been combined with cameras in order to increase the field of view (Rees, 1971, as cited by Nayar) for television applications. After 20 years catadioptric devices were introduced in robotics (Yagi et al., 1994) also to increase the field

of view. Nayar (1997) gave the first formal treatment of catadioptric systems with a single viewpoint in the context of computer vision. Visual sensors with a very big, close to hemi-spherical field of view, are called omnidirectional or panoramic. They are used in many application areas, including navigation, surveillance, and visualization. For a broad coverage of the field the reader is referred to an extensive review by Yagi (1999) as well as to the proceedings of the Workshop for Omnidirectional vision (Daniilidis, 2000) and to an upcoming book (Benosman and Kang, 2000).

In nature, most species with lateral eye placement possess an almost spherical field of view. In photography and machine vision, wide-angle field of view can be achieved with pure dioptric elements like fish-eye lenses (Shah and Aggarwal, 1996). Fish-eye lenses suffer from distortions for which explicit models have not been well-studied. Omnidirectional sensing can be realized also with a rotating camera (Shum and Szeliski,

2000). Rotating cameras are not suitable for dynamic scenes because they cannot cover actions in all directions simultaneously. The highest spatial resolution is given with a cluster of cameras pointing outwards (Swaminathan and Nayar, 2000). However, it is technically difficult to achieve a single effective viewpoint with a cluster of cameras.

Here we describe only omnidirectional work involving catadioptric sensors. We believe that the use of reflective components enables more degrees of freedom in the design of the sensor's geometric and optical properties. We classify the catadioptric systems in two groups, central and non-central, based on the uniqueness of an effective viewpoint; those having a single effective viewpoint are central catadioptric sensors. Non-central systems based on spherical (Bogner, 1995; Hong et al., 1991) or conical mirrors (Zheng and Tsuji, 1992) violate the single viewpoint constraint. Other non-central catadioptric systems are the mirror preserving ratios of elevations of points from a ground plane (Chahl and Srinivasan, 1997) or the mirror (Hicks and Bajcsy, 2000) which rectifies planes perpendicular to the optical axis.

Uniqueness of an effective viewpoint is desirable because it allows the mapping of any part of the scene to a perspective plane without parallax. In this sense, a central catadioptric system has the same effect as a rotating camera. Furthermore, easily modified multiple view algorithms can be applied for reconstruction (Taylor, 2000; Sturm, 2000). Nayar (1999) gave an extensive treatment of central catadioptric systems whose geometry can also be found in Svoboda et al. (1998), Bruckstein and Richardson (2000). Such systems are extensively used now for visualization (Boult, 1998; Onoe et al., 1998) and navigation (Winters et al., 2000; Leonardis and Jogan, 2000; Benosman et al., 2000). Nayar (Nayar and Peri, 1999) proved that folding mirrors with a conic profile can also yield a single effective viewpoint and a more compact mount. A folded catadioptric system consisting of two parabolic mirrors attached on a glass block has been designed by Greguss (1985) and used for surveillance in Zhu et al. (2000). Pyramidal multi-faceted mirrors mounted above clusters of cameras can simultaneously achieve high-resolution and one effective viewpoint (Nalwa, 1996; Majumder et al., 1999).

Our work deals with the geometric properties of central catadioptric sensors and is related to the work (Svoboda et al., 1998; Nene and Nayar, 1998) where it is shown that lines project onto conic sections.

Regarding calibration, a two-view algorithm not related to our approach has been proposed by Kang (2000). Regarding geometry, we use well-known facts from the mappings of the projective plane to the sphere. In computer graphics and vision, such mappings have been explicitly used in the context of oriented projective geometry as described by Stolfi (1991) and applied in Laveau and Faugeras (1996), Pajdla et al. (1998), Hartley (2000).

Our motivation to study central catadioptric cameras is to understand the geometric properties of the mappings realized with these sensors. The fact that we are able to choose the parameters of a quadric mirror surface and appropriately mount the camera implicitly encodes information which should be exploited during image interpretation.

In this paper we show that there is an equivalence between any central catadioptric projection and a composite mapping through the sphere. This mapping consists of the projection of a point from the center onto the sphere and a subsequent projection from a point on the axis of the sphere onto a plane perpendicular to that axis. The position of the point on the axis depends on the shape of the mirror. When the point lies between the north-pole and the center the composite mapping is equivalent to a projection induced by a hyperbolic mirror and a perspective camera. The extrema of this interval yield the following interesting cases:

1. An orthographic camera with a parabolic mirror which is equivalent to the projection on the sphere with a subsequent projection from the north pole to the plane through the equator. This latter projection is well known as the stereographic projection and is a conformal mapping.
2. A perspective camera combined with a planar mirror which can be modeled as a projection on the sphere with a subsequent projection from the center to the plane tangent at the south-pole.

In the course of proving this equivalence we have also been able to establish a unifying formula covering all of the cases above.

Once proven, the equivalence paves a ground for building up a geometry based on the intermediate representation on the sphere. It is well known that point-line duality of the projective plane maps to the point-great circle duality on the sphere. Through the equivalence it is trivial to observe that lines in space project onto great circles on the sphere and subsequently onto conic

sections on the plane. Thus, line images (great circles on the sphere and conic sections on the catadioptric plane) are dual to points (poles of great circles). The new fact we prove in this paper is that there is also a duality between catadioptric projections and hence also mirror shapes: If a mirror shape *s* projects a line in space to a conic, there exists a dual shape *s'* which projects the normal of the plane containing the line to the foci of the conic. It turns out that the parabolic catadioptric projection is dual to the perspective projection: the parabolic projection of a line is a circle whose center is the perspective projection of the normal of the plane containing the line.

The first practical implication of the proved equivalence is the intrinsic calibration of a catadioptric system. We assume that the unknown parameters are the combined focal length of the camera and the mirror, the eccentricity of the conic section of the mirror, and the image center. By enumerating the constraints given by the line images (lines in perspective, circles in parabolic, conics in hyperbolic and elliptic cases) we explain how we are able to calibrate from a single view of arbitrary lines in the parabolic, hyperbolic, and elliptic cases but not in the case of a conventional perspective camera. We outline an algorithm for the parabolic case and apply it on a commercially available catadioptric camera.

In the next section we provide a purely geometric proof of the equivalence of parabolic projection and stereographic projection of the projective plane when represented as a sphere. In Section 3 we prove the generalization of the equivalence to all central catadioptric systems. We present the novel duality relationships in Section 4. Finally we conclude with the implications on calibration.

2.   A Geometric Introduction

Let us begin with the parabolic case. In the time of Apollonius, the Greek astronomer Diocles was asked by Zenodorus, "how to find a mirror surface such that when it is placed facing the sun the rays reflected from it meet a point and thus cause burning," (Toomer, 1976). Diocles responded that such a surface is the parabola. Computer vision practitioners are typically not interested in burning but in seeing. A convex, reflective parabolic mirror placed above and parallel to the axis of an orthographically projecting camera results in a sensor with a single effective viewpoint at the focus of the parabola. It is therefore equivalent to a purely rotating perspective camera. A ray of light incident with the focus of the parabola is reflected by the mirror to a ray of light parallel to its axis (see Fig. 1).
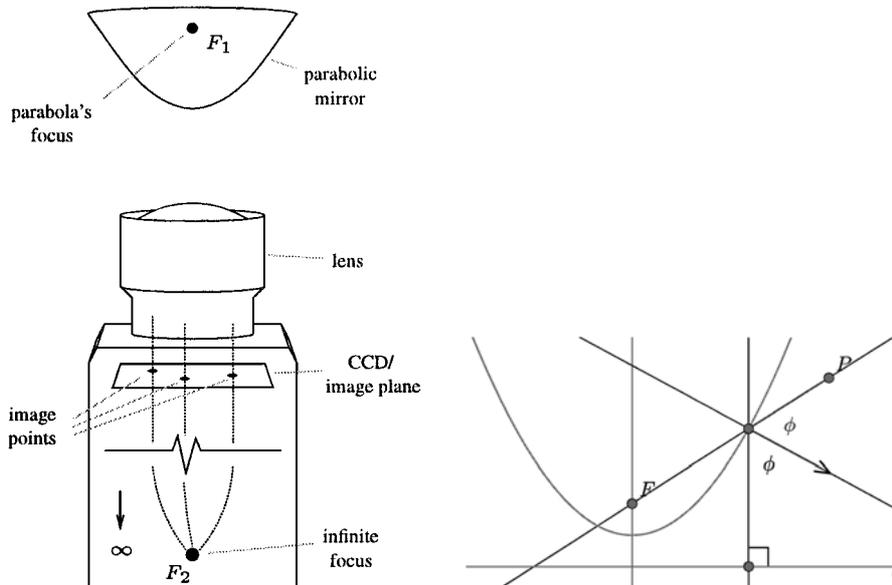

Figure 1.   On the left is a diagram showing the configuration of a typical parabolic catadioptric sensor. A parabolic mirror is placed in front of a camera approximating an orthographically projecting lens (one whose focus is at infinity). The right diagram is a further abstraction of the left and shows that a ray of light incident with the focus of the parabola is reflected to a ray of light parallel to the parabola's axis.
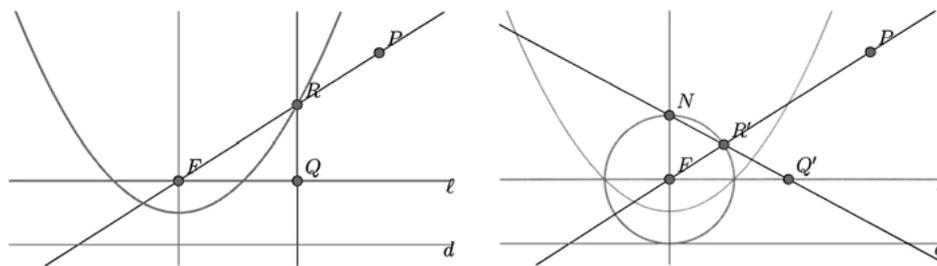
Figure 2.   Left: diagram corresponding to Definition 1. Right: diagram corresponding to Definition 2.

Thus, every point in the image is in one-to-one correspondence with a ray originating at the focus.

In the process of developing a calibration algorithm for these devices (Geyer and Daniilidis, 1999), we discovered that the projections of lines are a certain class of circles. The class is defined by the property that each and every one of these circles intersects a single circle, the fronto-parallel horizon, antipodally—except for this single circle which is itself a member of this class. Upon further reflection we recalled stereographic projection of the sphere and its property that it projects circles, great or small, on the sphere to circles in the plane. In particular, it sends great circles, all of which intersect the equator antipodally, to circles which intersect the projection of the equator antipodally. The sphere is just one representation of the projective plane, in which, lines in space project to great circles. It is therefore natural to suspect that these two projections are somehow equivalent.

We now go about proving the equivalence of parabolic projection and stereographic projection of the projective plane. The parabolic mirror is a regular paraboloid and because the one-to-one mapping is preserved in a plane through the paraboloid's axis, we need only consider a cross-section of the paraboloid.

Let us assume the existence of a parabola p with focus F and directrix d (see Fig. 2 left). The directrix and the focus define the parabola: all points on the parabola are equidistant to the directrix and the focus. Let ℓ be perpendicular to the axis of p and through F. Consider the following definition of the projection Q of a point P, reflected by the parabola, to the line ℓ.

Definition 1. Q is the projection of the point R to the line ℓ, where R is the intersection of the parabola and the ray FP.

We now give an alternative definition. Let a circle have center F and radius equal to twice the focal length

of the parabola. The circle and parabola intersect twice on the line ℓ and the directrix is tangent to the circle (see Fig. 2 right). Let N be the point diametrically opposite to the intersection of the circle with the directrix, this is the north pole of the circle. We claim the following definition is also equivalent. This definition is the basis for our generalization to arbitrary catadioptric projections.

Definition 2. Q' is the projection of the point R' to the line ℓ from the point N, where R' is the intersection of the ray FP and the circle.

The first step of Definition 2 is to project points to the circle from its center. This is equivalent to the projection from the projective plane to the projective line, which is represented as a circle here. The second step is the two dimensional equivalent of stereographic projection—project from the "north pole" of the circle to a line perpendicular to the axis of the circle. We prove the following lemma.

Lemma 1.   *The parabolic projections of a point P, given in Definitions 1 and 2, respectively yield points Q and Q' which are coincident.*

Proof: Choose a point P in the plane. Intersecting the ray FP with the circle we obtain R'; intersecting with the parabola we obtain R. Let Q' be the projection of R' from the point N to the line ℓ perpendicular to the axis NF at F. Let Q be the orthographic projection of R to the line ℓ. Let Y be the intersection of the directrix and the circle. Finally let C be the intersection of the lines RQ and NQ', and let X be the intersection of the lines RQ and d, the directrix. To prove that the projections are equivalent we need to show that Q equals Q'. We do so by first showing that $|CX|$ equals $|QX|$. This would imply that $Q = C$, since Q and C lie on the same line; and therefore also that $Q = Q'$, since C is on the
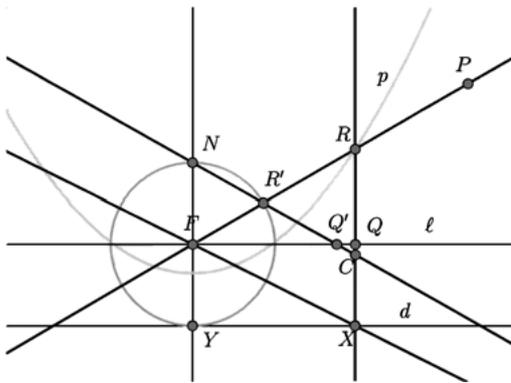
Figure 3.   A proof by contradiction. Assume that the points Q and Q' are not equal. The diagram is *intentionally drawn incorrectly*; the parabola is drawn as a hyperbola so that Q and Q' do not coincide.

line ℓ and Q' is defined to be the intersection of NR' with ℓ.

Assume that Q is not equal to Q' and that Q is not equal to C (if Q is equal to C then Q, Q' and C are equal as discussed above); see Fig. 3. By the definition of the parabola the point R is equidistant to the directrix and the focus. Therefore the triangle FRX is isosceles. Because R' and N lie on a circle whose center is F, the triangle $R'FN$ is isosceles. This triangle is similar to $R'RC$ because the parabola's axis is parallel to RX. Since both $R'RC$ and FRX are isosceles, $R'C$ must be parallel to FX, and thus $|CX|$ equals $|R'F|$. Then $|CX|$, $|FY|$, $|R'F|$, and $|Q'X|$ are all equal. In particular $|CX| = |Q'X|$, but C and Q' lie on the line above the directrix, and therefore above the point X in the figure. If they lie on the same side of a line with respect to some point and have the same distance to this point then they must be the same point. But this is a contradiction because we assumed that the points were not equal.   □

Discussion.   The two definitions above can easily be extended to three dimensions, and so may the lemma be extended, and thus projection by a parabolic mirror is equivalent to projection to the sphere followed by stereographic projection. We now wish to know if there is a generalization. Recall that perspective projection may also be obtained via a projection of a sphere; first project to the sphere from the center, second, project from the center to the image plane. The separation into two steps is unnecessary because the projections are both from the same point. But notice that the first step is the same as in the equivalent parabolic projection via

the sphere. The difference in the second steps are only the point on the sphere's axis from which to project to the image plane. What is the effect of changing the point of projection to a point that is neither the north pole, nor the sphere center? Is it possible to model hyperbolic mirrors by appropriately choosing this second projection center? The answer is yes; if we choose an appropriate point on the axis, between the north pole and the sphere's center, we obtain a projection equivalent to a hyperbolic projection, as well as an elliptic projection where the ellipse's eccentricity is the reciprocal of the hyperbola's.

Is there any advantage to this representation? We claim that there is. First, it is a unifying representation in that it includes perspective, parabolic, hyperbolic, and elliptic projections. Additionally, the sphere is a standard representation of the projective plane; this proves that there is a simple mapping, in fact a central projection, from a standard representation of the projective plane to a projective plane induced by any central catadioptric projection. With this representation it is easy to determine the projections of lines, and also leads to the discovery of a novel duality relationship. Without this model it is not clear (to us) that parabolic projection is conformal, which is trivially implied by its equivalence with stereographic projection. We would hope that this representation leads to a greater understanding of and less hesitation in using catadioptric devices (due to the perceived additional complexity of curved intermediary reflective surfaces).

In the next section, we prove and explore the generalization. We develop the general theory in the context of projective geometry. We use homogeneous coordinates and constructively utilize the relevant Euclidean property, namely that a ray incident with one focus is reflected to a ray incident with the second.

Finally, we add that we are not the first to discover a relationship between stereographic projection and the parabola. During a revision of our paper we discovered the work of Penrose and Rindler (1984) in which they imagine a point and the movement of a plane in space. At time $t = 0$, the point emits a flash of light isotropically, and at the same instant, the plane starts moving toward the point at the speed of light. The locus of points traced out by the intersection of the plane and the sphere of light emanating from the point is a paraboloid whose focus is the light source. They prove that a given point on the ever expanding sphere meets the plane at the same point where it would have been projected stereographically from the unit sphere.

3. Central Catadioptric Projections

In this section we prove the extension of the equivalence to arbitrary catadioptric projections and a map similar to stereographic projection. Before proving this extension we introduce quadratic projections (which serves as a context in which we provide a proof). We prove the equivalence for a two-dimensional catadioptric projection in Lemma 1. The lemma immediately yields an extension to three dimensions with which we obtain the main result in Theorem 1 as well as several corollaries. We then discuss the nature of the images of points and lines and how they create catadioptric projective planes. Throughout this paper we assume that mirrors are ideal, the cameras satisfy the pinhole camera model, and both are properly aligned with respect to one another. We only consider non-degenerate catadioptric configurations, namely planar, parabolic, hyperbolic and elliptic cases. Neither of the degenerate cases, the conic and spherical cases, are of practical use as single effective viewpoint sensors. As shown in Baker and Nayar (1998) these are the *only* catadioptric devices with a single effective viewpoint.

Catadioptric projections are a subset of a general type of projection. In a central catadioptric projection, a point is first projected to a conic from one of the foci and then this point is projected to an image plane from the second focus (see Fig. 4). We could instead choose different points from which to project and different surfaces to intersect but these configurations may not induce optical projections which coincide with the abstract projections. Note that in the previous section,
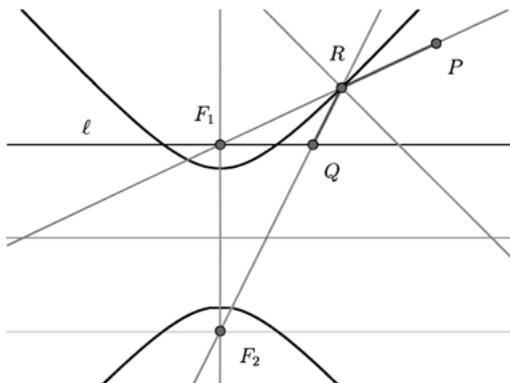

Figure 4. In general a conic reflects any ray of light incident with one of its foci (here F_1) to a ray of light incident with its other focus (F_2). Central catadioptric devices utilize this property and achieve a single effective viewpoint at one of the foci of a conic (F_1).

we found a surface, namely the sphere, and a pair of points, the sphere center and its north pole, which gave a projection equivalent to an optical projection, namely parabolic projection.

We define a general mapping which consists of a composition of two projections. The first projection is to a quadric or conic from a point. The second projection is to a plane or line from a second point. We call these quadratic projections. In the definition below we restrict ourselves to two dimensions, but it may be easily extended to three or an arbitrary number of finite dimensions. We use the notation $A \vee B$ to mean the line joining points A and B, and $l \wedge m$ to mean the point lying on both lines l and m. For notational convenience we have overloaded these operators to include quadratics, so that $l \vee q$, where l is a line and say q is a conic, to mean the two points of intersection of the line with the conic. Finally, when the intersection is a pair, we distribute over other applications of $\vee$ and $\wedge$, i.e. $A \vee (l \wedge q)$ is the pair $(A \vee P_1, A \vee P_2)$, where $P_{1,2}$ are points obtained from the intersection of l and q.

Definition of a quadratic projection.   Let c be a conic, let A and B be two arbitrary points, and let ℓ be any line not containing B. Choose a point P. The intersection of a line and a quadric is two, possibly imaginary, points, so let R_1 and R_2 be the intersection of c with AP, imaginary or not. Then R_1 is one of the projections of the point P to the conic c, R_2 is the second. Now project the R_i's to the line ℓ from point B. Let Q_i be the intersection of BR_i with ℓ. The Q_i's are the quadratic projections of the point P to the line ℓ. We call this map $q(c, A, B, \ell) : \mathbb{P}^2 \to \pi_\ell$ where π_ℓ is the projective line induced on the line ℓ in which points such as Q_1 and Q_2 are identified. We may write the map as

$$P \stackrel{q(c,A,B,\ell)}{\longrightarrow} (((P \vee A) \wedge c) \vee B) \wedge \ell \,.$$

In the three dimensional case, the conic becomes a quadric surface and ℓ is replaced by a plane, inducing a projective plane. Note that any map $q(c, A, B, \ell)$ has a single effective viewpoint at A, at least in the sense that only rays through A are intersected with c; this, however, may not correspond to an optical projection, where the angle of incidence with c is equal to the angle of reflection.

A subset of the quadratic projections are catadioptric projections which not only have a single effective viewpoint but also in which the angle of incidence with c is equal to the angle of reflection. This occurs

when the two points of projection are the foci of the conic.

Definition of a catadioptric projection via quadratic projections. Let c be a conic whose foci are F_1 and F_2, where F_1 is finite and F_2 might lie on the line at infinity. Let ℓ be a line perpendicular[1] to $F_1 F_2$ but not containing F_2. A catadioptric projection is the quadratic projection $q(c, F_1, F_2, \ell)$.

Catadioptric projections may similarly be extended to three dimensions. Note that in the case where c is a degenerate line conic having two foci $F_{1,2}$ whose perpendicular bisector is the line conic, and ℓ coincides with the line conic, then $q(c, F_1, F_2, \ell)$ is perspective projection with viewpoint F_1 and focal length $\frac{1}{2}\overline{F_1 F_2}$. When c is a parabola, F_1 its finite focus, F_2 its focus on the line at infinity, and ℓ the line perpendicular to the axis of c and through F_1, then $q(c, F_1, F_2, \ell)$ is the parabolic projection defined in Definitions 1 and 2.

Given a catadioptric projection with parameters (c, F_1, F_2, ℓ), what is the set of parameters (c', A, B, ℓ') yielding equivalent quadratic projections? We do not attempt to answer this question in general, however we answer a constrained form of the question. Are there parameters (c', A, B, ℓ'), where c' is a unit-radius circle centered at A, B is some point, and $\ell' \parallel \ell$, which yield equivalent projections? It is clear that in order for the projections to be the same they must have the same single effective viewpoint, and therefore $A = F_1$. Hence, we wish to find ℓ' and B such that

$$q(c, F_1, F_2, \ell) = q(c', F_1, B, \ell'),$$

where c' is a circle centered at F_1 with unit radius. For example, in Section 2 we showed that if c is a parabola, F_1 is the focus, F_2 is the point at infinity lying on the axis of the parabola, i.e. the parabola's infinite focus and the focal point of an orthographic projection, and ℓ is perpendicular to the axis at F_1, then

$$q(c, F_1, F_2, \ell) = q(c', F_1, N, \ell),$$

where c' is a circle centered at F_1 and whose radius is equal to twice the focal length of the parabola, and where N is the point on the circle diametrically opposite the point tangent to the directrix (the circle and directrix are tangent). We give then the following lemma.

Lemma 2. *Let $q(c, F_1, F_2, \ell)$ be a catadioptric projection, F_i are the foci of c and ℓ is the image line. There exists a unit circle c' centered at F_1, a point B, and a line ℓ', $\ell' \parallel \ell$, such that*

$$q(c, F_1, F_2, \ell) = q(c', F_1, B, \ell'),$$

up to translation from ℓ' to ℓ.

Proof: We prove the lemma by first deriving the formula for the catadioptric projection $q(c, F_1, F_2, \ell)$, then deriving the spherical projection formula $q(c', F_1, B, \ell')$, equating them and solving for the position of B, and the position of the intersection of ℓ' with the y-axis. We see that the parameters ℓ' and B are independent of the choice of the point to project.

Step 1: Derivation of $q(c, F_1, F_2, \ell)$. We assume without loss of generality that $F_1 = (0, 0, 1)$ and that the quadratic form of c, in terms of its eccentricity ϵ and a scaling parameter $\lambda > 0$, is as follows:

$$\mathbf{Q}_{\epsilon,\lambda} = \begin{pmatrix} 4 & 0 & 0 \\ 0 & 4 - 4\epsilon^2 & -4\epsilon\lambda \\ 0 & -4\epsilon\lambda & -4\lambda^2 \end{pmatrix}.$$

Then F_1 and $F_2 = (0, -2\epsilon, \lambda^{-1}(\epsilon^2 - 1))$ are the foci of c whose latus rectum is 2λ. Recall that the latus rectum is the length of the line segment created by the two points of intersection of the conic c and line ℓ. Also assume that the y-intercept of the line ℓ is μ, so that the line has coordinates $[0, 1, -\mu]$. Note that this parameterization includes perspective projection with planar mirror in the limit as $\epsilon \to \infty$ as long as we set $\lambda = 2f\epsilon^{-1}(\epsilon^2 - 1)$ and $\mu = -3f$, and divide $Q_{\epsilon,\lambda}$ by $1 - \epsilon^2$.

We now find the projection $q(c, F_1, F_2, \ell)$ of P. First, the points R_1 and R_2 in $(P \vee F_1) \wedge c$, being the intersection of a line and a conic, may be expressed as

$$R_i = F_1 + \theta_i P,$$

for some $\theta_1, \theta_2 \in \mathbb{C}$, where these θ_i are roots of a quadratic equation. We obtain the quadratic equation from the condition that R_i lies on the conic,

$$\begin{aligned} 0 &= R_i \mathbf{Q}_{\epsilon,\lambda} R_i^T \\ &= (F_1 + \theta_i P) \mathbf{Q}_{\epsilon,\lambda} (F_1 + \theta_i P)^T \\ &= F_1 \mathbf{Q}_{\epsilon,\lambda} F_1^T + 2\theta_i F_1 \mathbf{Q}_{\epsilon,\lambda} P^T + \theta_i^2 P \mathbf{Q}_{\epsilon,\lambda} P^T. \end{aligned}$$

Therefore,

$$\theta_i = \frac{-2F_1\mathbf{Q}_{\epsilon,\lambda}P^T + (-1)^i\sqrt{4(F_1\mathbf{Q}_{\epsilon,\lambda}P^T)^2 - 4(P\mathbf{Q}_{\epsilon,\lambda}P^T)(F_1\mathbf{Q}_{\epsilon,\lambda}F_1^T)}}{2P\mathbf{Q}_{\epsilon,\lambda}P^T} = \frac{\lambda}{(-1)^i\sqrt{x^2+y^2}-\epsilon y-\lambda w},$$

when $P = (x, y, w)$ (no z since we are considering the projection restricted to the plane). So the points

$$\begin{aligned}
R_i &= F_1 + \theta_i P \\
&= F_1 + \frac{1}{(-1)^i\sqrt{x^2+y^2}-\epsilon y - w}P \\
&= \begin{pmatrix} \frac{\lambda x}{(-1)^i\sqrt{x^2+y^2}-\epsilon y-\lambda w} \\ \frac{\lambda y}{(-1)^i\sqrt{x^2+y^2}-\epsilon y-\lambda w} \\ 1 + \frac{\lambda w}{(-1)^i\sqrt{x^2+y^2}-\epsilon y-\lambda w} \end{pmatrix}^T.
\end{aligned}$$

Next we project the R_i to the line $\ell = [0, 1, -\mu]$ from the point F_2. This transformation is expressed as the matrix

$$\mathbf{T}_{\epsilon,\lambda,\mu} = \begin{pmatrix} -2\epsilon\lambda + \mu(1-\epsilon^2) & 0 \\ 0 & (1-\epsilon^2) \\ 0 & -2\epsilon\lambda \end{pmatrix}.$$

The projected points Q_i are then given by projective line coordinates

$$\begin{aligned}
Q_i &= R_i\mathbf{T}_{\epsilon,\lambda,\mu} \\
&= (x(2\epsilon\lambda - \mu(1-\epsilon^2)), \\
&\quad -(1+\epsilon^2)y - 2(-1)^i\epsilon\sqrt{x^2+y^2}), \quad (1)
\end{aligned}$$

and $q(c, F_1, F_2, \ell) = \{Q_1, Q_2\}$.

Step 2: Derivation of $q(c', A, B, \ell)$. Now find the spherical projection, or in the cross-section, the projection to the circle. Let c' be the unit circle centered at F_1. The points R_i', which are the intersections of the line F_1P with this circle, may be found without difficulty due to the simplicity of the circle, all that is necessary is a normalization. In particular

$$R_i' = (x, y, (-1)^i\sqrt{x^2+y^2}).$$

Now we must determine the projection of the points R_i' to the image line ℓ'. The projection is just a perspective transformation from the unknown point B. By symmetry the point B lies on the line F_1F_2, we therefore parameterize B with l, writing $B = (0, l, 1)$. Then the matrix projecting a point to the line $\ell' = [0, 1, -m]$ from B may be expressed as

$$\mathbf{U}_{l,m} = \begin{pmatrix} l-m & 0 \\ 0 & -1 \\ 0 & l \end{pmatrix}.$$

Thus,

$$\begin{aligned}
Q_i' &= R_i'\mathbf{U}_{l,m} \\
&= ((l-m)x, -y + l(-1)^i\sqrt{x^2+y^2}) \quad (2)
\end{aligned}$$

so that $q(c', F_1, B, \ell) = \{Q_1', Q_2'\}$.

Step 3: For what B and ℓ' is $q(c, F_1, F_2, \ell) = q(c', F_1, B, \ell')$? If l and m can be chosen independently of x, y, and w such that Eqs. (1) and (2) are equal (up to a scale, remember that we work in homogeneous coordinates), then we have shown that the two projections are equivalent. This is indeed the case, and if we choose

$$\begin{aligned}
l &= \frac{2\epsilon}{1+\epsilon^2}, \\
m &= \frac{\mu - \epsilon(\epsilon\mu + 2\lambda - 2)}{1+\epsilon^2},
\end{aligned}$$

then substituting in (2) gives

$$\left(\frac{(2\epsilon\lambda - \mu + \epsilon^2\mu)x}{1+\epsilon^2}, 0, -y + \frac{2(-1)^i\epsilon\sqrt{x^2+y^2}}{1+\epsilon^2}\right).$$

Multiply this by $1 + \epsilon^2$ and we obtain

$$\begin{aligned}
&(x(2\epsilon\lambda - (1-\epsilon^2)\mu, 0, -(1+\epsilon^2)y \\
&\quad + 2(-1)^i\epsilon\sqrt{x^2+y^2}),
\end{aligned}$$

which is the same as (1). Therefore

$$q(c, F_1, F_2, \ell) = q(c', F_1, B, \ell')$$
$$= q\left(\odot (F_1; 1), F_1, \left(0, \frac{2\epsilon}{1 + \epsilon^2}, 1\right),\right.$$
$$\left. \left[0, 1, -\frac{\mu - \epsilon(\epsilon\mu + 2\lambda - 2)}{1 + \epsilon^2}\right] \right),$$

up to scale.   □

Extension to three dimensions.   We can now extend the definition to three dimensions. We assume that c is rotationally symmetric about the z-axis having only two foci F_1 and F_2 with coordinates $(0, 0, 0, 1)$ and $(0, 0, -2\epsilon, \lambda^{-1}(\epsilon^2 - 1))$, and that p is the plane $[0, 0, 1, -\mu]$. Then,

$$q(c, F_1, F_2, p) = q\left(\odot (F_1; 1), F_1, \left(0, 0, \frac{2\epsilon}{1 + \epsilon^2}, 1\right),\right.$$
$$\left. \left[0, 0, 1, -\frac{\mu - \epsilon(\epsilon\mu + 2\lambda - 2)}{1 + \epsilon^2}\right] \right),$$

up to scale, where $\odot(F_1; 1)$ is the sphere centered at F_1 with a radius of 1.

Definition of a spherical projection.   A spherical projection is the composition of central projection to the unit sphere followed by projection from a point on some axis of the sphere a distance l from the sphere's center to a plane perpendicular to the axis a distance m below the center and is represented by the quadratic projection

$$s_{l,m} = q(\odot(A; 1), A, (0, 0, l, 1), [0, 0, 1, m]);$$

note that we have changed the sign of m.

Lemma 2, and its extension to three dimensions, is the main contribution of this paper. It shows that there exists a point B such that the projection through the sphere is equivalent with the given catadioptric projection. Having now defined a spherical projection, we summarize the specific results in the following theorem in terms of spherical projections. The theorem uses the point B constructed in the lemma. Afterwards we give corollaries which follow immediately from the theorem.

Theorem 1 (*Projective Equivalence*). *All non-degenerate central catadioptric projections are equiv-alent to a central projection of the spherical representation of the projective plane to a plane. All such projections can be represented with the single map $s_{l,m}$, where the parameter l is a function of the eccentricity of the conic and m is a function of both its scale and eccentricity. Unless stated otherwise, $\mu = 0$ and $\lambda = 2p$. We enumerate the possible cases in parallel with Fig. 5:*

1. *$0 < \epsilon < 1$. Elliptic projection is equivalent to the composition of normalization to the unit sphere and central projection:*

$$q(c, F_1, F_2, p) = s_{\frac{2\epsilon}{1+\epsilon^2}, \frac{2\epsilon(2p-1)}{1+\epsilon^2}},$$

   where c is an ellipse of eccentricity ϵ whose latus rectum is $4p$, and foci are $F_1 = (0, 0, 0, 1)$ and $F_2 = (0, 0, 4p\epsilon, \epsilon^2 - 1)$, and where $p = [0, 0, 1, 0]$.

2. *$\epsilon = 1$. Parabolic projection is equivalent to the composition of normalization to the unit sphere followed by stereographic projection:*

$$q(c, F_1, F_2, p) = s_{1, 2p-1},$$

   where c is a parabola whose latus rectum is $4p$, and foci are $F_1 = (0, 0, 0, 1)$ and $F_2 = (0, 0, 1, 0)$, and where $p = [0, 0, 1, 0]$.

3. *$\epsilon > 1$. Hyperbolic projection is equivalent to the composition of normalization to the sphere followed by central projection:*

$$q(c, F_1, F_2, p) = s_{\frac{2\epsilon}{1+\epsilon^2}, \frac{2\epsilon(2p-1)}{1+\epsilon^2}},$$

   where c is a hyperbola whose latus rectum is $4p$, and foci are $F_1 = (0, 0, 0, 1)$ and $F_2 = (0, 0, 4p\epsilon, \epsilon^2 - 1)$, and where $p = [0, 0, 1, 0]$.

4. *$\epsilon \to \infty, \lambda = 2f\epsilon^{-1}(\epsilon^2 - 1), \mu = -3f$. Perspective projection with focal length f in front of a planar mirror a distance of $2f$ from the focus is equivalent to normalization to the sphere followed by central projection:*

$$q(c, F_1, F_2, p) = s_{0, f}$$

   where c is the degenerate conic consisting of the single line $[0, 0, 1, 2f]$ (with a multiplicity of two) having foci $F_1 = (0, 0, 0, 1)$ and $F_2 = (0, 0, -4f, 1)$, and where $p = [0, 0, 1, 3f]$.
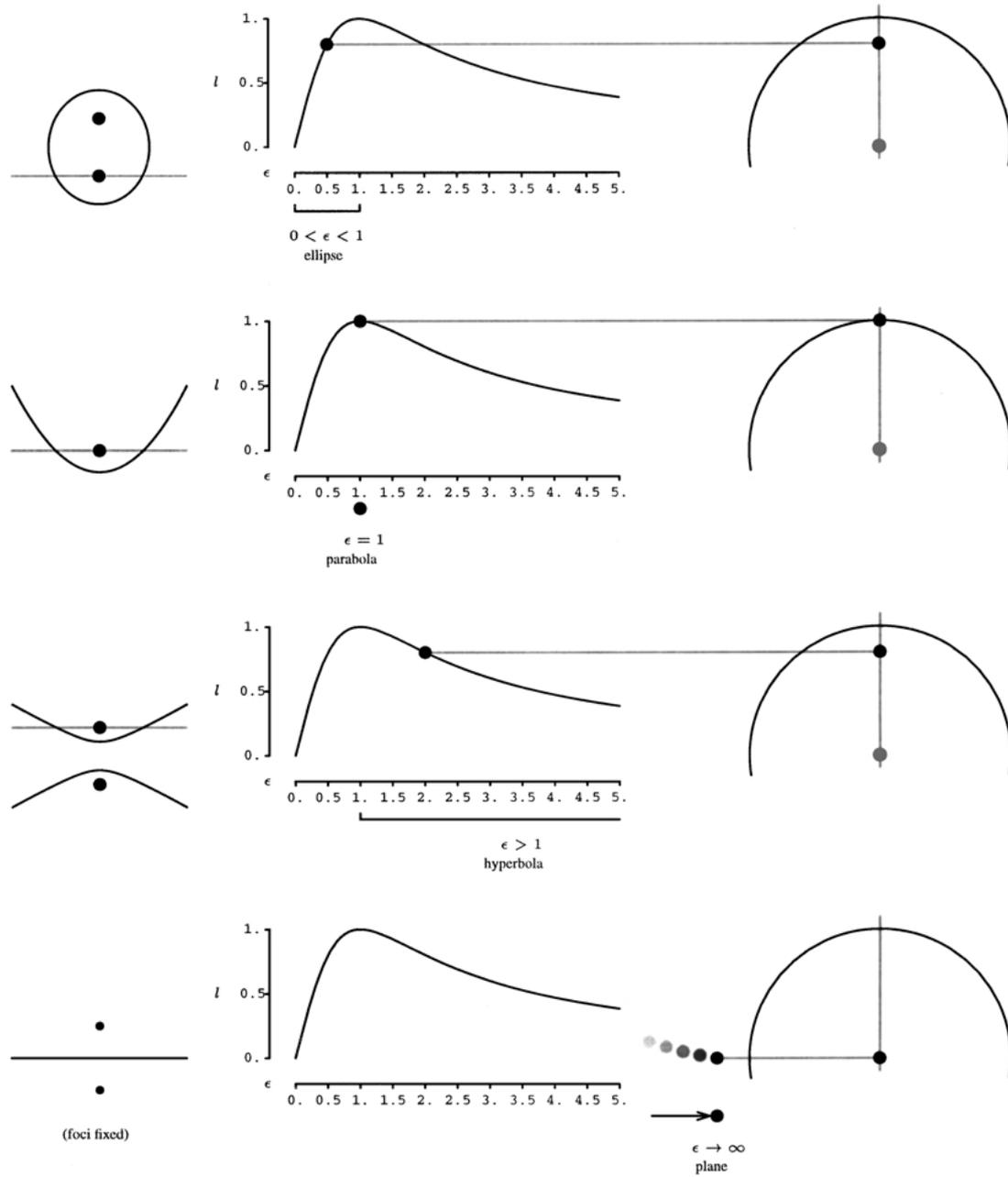
232   *Geyer and Daniilidis*

Figure 5. The different catadioptric projections and the corresponding positions of the second projection center on the axis of the sphere in the equivalent projection. In the elliptic and hyperbolic cases (top and second to bottom) the corresponding point lies between the north pole and the center of the sphere. In the parabolic case, the second projection point is the north pole; in the perspective case the center is the second projection center, which is obtained in the limit as the eccentricity goes to infinity. The graph in the second column shows the height of the second projection center as a function of eccentricity. Note that for a given height between the north pole and the center there is an elliptic mirror and a hyperbolic mirror equivalent to the projection induced with this point as the second projection point.

Corollaries.

1. *Parabolic projection is conformal. The angles between great circles on the spherical representation of the projective plane are preserved in the parabolic projective plane. For example, the horizons of two perpendicular planes are two orthogonal circles. This is because stereographic projection is conformal (Needham, 1997).*

2. *Conformal maps on the sphere project to conformal maps in the parabolic projective plane. In particular, pure rotations of space preserve the angles between great circles, and thus rotations of space preserve angles in the parabolic projective plane.*

3. *Catadioptric projections with reciprocal eccentricities are projectively equivalent; such projections have the same representation, for if $\epsilon = \epsilon'^{-1}$, then*

$$l' = \frac{2\epsilon'}{1 + \epsilon'^2} = \frac{2\frac{1}{\epsilon}}{1 + \left(\frac{1}{\epsilon}\right)^2} = \frac{2\epsilon}{1 + \epsilon^2} = l.$$

This implies that any elliptic catadioptric device is projectively equivalent to a hyperbolic projection. We therefore need only consider one of these cases, and we arbitrarily choose to refer to such projections as hyperbolic.

3.1.   Point Images

The sphere, in which antipodal points are identified, is just one representation of $\mathbb{P}^2$; Stolfi (1991) calls this the spherical model or representation. The "points" of $\mathbb{P}^2$ in this representation are the antipodal point pairs, and the "lines" in this representation are the great circles. Any two non-identical lines—great circles—intersect in a point pair. There is a single line joining any two non-identical point pairs. The plane adjoined with the line at infinity is another representation in which the "points" are the single points of the plane and the line at infinity; this is the so called "straight model." Homogeneous coordinates, the analytic model, are yet another representation in which the "points" are rays through the origin in $\mathbb{R}^3$. These are all interrelated and equivalent, and for example the straight model is obtained from the spherical one by central projection from the center of the sphere.

The straight model is a natural model for studying perspective cameras but not so natural for studying general catadioptric cameras. Now that we have shown that catadioptric projections are obtained from the spherical model by a central projection, it is only natural to study a different representation, one obtained by central projection from a point on the axis of the sphere. The question is this: What geometric structures which preserve the incidence relationships of $\mathbb{P}^2$ are induced by such a central projection?

For example, as we just noted, the straight model is obtained from the spherical one by central projection from the sphere's center to a plane tangent to the sphere. The lines of the straight model are just that, lines in the plane. However, in order to preserve the axioms of projective geometry, we needed to add the line at infinity so that two parallel lines "intersect", as required by the axioms.

In a model obtained by central projection from some other point we need to define the "points" and the "lines" that make up the representation. Then we need to add the necessary structure to satisfy the axioms. In this section we consider the projections of points; in the next we determine the projections of lines. Lastly, we summarize the structure of these new representations, the *catadioptric projective planes*.

We will let the projective planes induced by the catadioptric projections consist of point pairs corresponding to points in $\mathbb{P}^2$ and subsets of these point pairs corresponding to lines of $\mathbb{P}^2$ which are actually conic sections. The representation of a single point in a pair is in homogeneous coordinates (with one exception in the parabolic case), but the homogeneous coordinates are only a setting, inadequate to fully describe the representation given in the catadioptric projective planes.

First the parabolic case. Prior to defining the points of the parabolic projective plane, we examine some of the properties of stereographic projection. In this case there is a one-to-one mapping between the sphere, minus the north pole, and the Euclidean plane. Points below the equator are mapped to points within the projection of the equator, i.e. the fronto-parallel horizon. Points above are sent to points outside this circle. The north pole does not have a projection in homogeneous coordinates, since the projection formula gives the point $(0, 0, 0)$. These are not valid homogeneous coordinates. Since we will want every "point" to consist of a pair, in order that the parabolic projective plane be complete, we add this additional point. Because the projection of no other point is degenerate, i.e. mapped to $(0, 0, 0)$, this is the

label we give it. Thus the range is not just $\mathbb{P}^2$, but $\mathbb{P}^2 \cup (0, 0, 0)$.

The "points" of the parabolic projective plane thus consist of the projections of the antipodal point pairs of S^2. Every point within the projection of the equator is paired with a point outside. The projection of the south pole is paired with the point $(0, 0, 0)$, corresponding to the north pole.

The hyperbolic case is more complicated. In this case as we have seen, the second center of projection is between the north pole and the center. Points on the sphere at a height below this second projection center are in one-to-one mapping with points of the plane. Points on the sphere at exactly the same height as the projection point are mapped to the line at infinity. Points on the sphere above the projection point are also in one-to-one correspondence with points of the plane. Thus the projection is not injective as it is in the parabolic case; it is actually a double covering. This is somewhat problematic; a solution is to keep two copies of the plane, one for the points above and one for the points below the point of projection, see Fig. 6. In practice, this is not necessary because the points lying above the projection point are points that would be reflected by the lower sheet of the two sheets of the hyperboloid. However, the lower sheet is not used when designing catadioptric sensors because this is where the camera is placed.

3.2. Line Images

It is now trivial to see that the image of a line in the general case is a conic: First the projection of a line
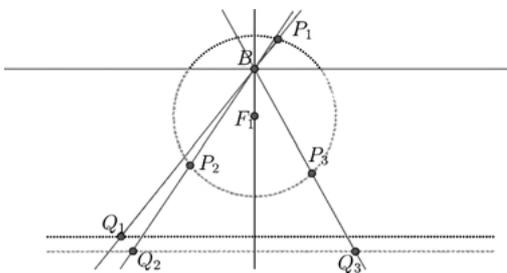

Figure 6. Points below the point B are projected to the lower copy of the plane; points above the point B are projected to the upper copy of the plane. Points at the same height as B are projected to the line at infinity. Notice that the images Q_1 and Q_2 are near each other but are respectively projected from points P_1 and P_2 which are not near each other.
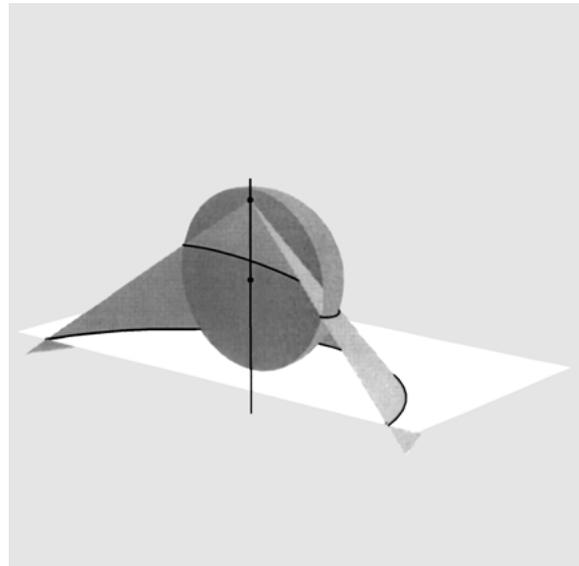

Figure 7. The projection of a line to the sphere is a great circle; the projection of the great circle is obtained from the intersection of the image plane with a cone containing the great circle and whose vertex is the point of projection.

in space to the sphere is great circle. There is a cone through the second center of projection and this great circle as in Fig. 7. The intersection of this cone with the image plane is the line image and is obviously a conic.

One special line image is the fronto-parallel horizon. This is the image of the equator. In the parabolic and hyperbolic cases it is clearly a circle centered at the image center with a radius dependent on the eccentricity and focal length. In the perspective case, the fronto-parallel horizon is the line at infinity. Thus, one of the effects of a catadioptric projection is bringing in from infinity the line at infinity. We will see later that this enables a calibration from lines.

The intersection of any great circle with the equator are two points antipodal on the equator. The projections of these two points are, in the hyperbolic and parabolic cases, two points antipodal on the fronto-parallel horizon. Thus, the intersection of any line image and the fronto-parallel horizon are two points antipodal on the fronto-parallel horizon.

Now we find an explicit formula for the quadratic form of a line image. We must first derive the quadratic form of the cone through the second projection center and the great circle. We then intersect that cone with the image plane to obtain the line image.

A cone is a special case of a quadric. In general a quadric is a set of points satisfying

$$PQP^T$$

$$= (x \ y \ z \ w) \begin{pmatrix} a & b & c & d \\ b & e & f & g \\ c & f & h & i \\ d & g & i & j \end{pmatrix} \begin{pmatrix} x \\ y \\ z \\ w \end{pmatrix} = 0.$$

We need to find the entries of $\mathbf{Q}$ given the unit normal $\hat{n} = (n_x, n_y, n_z)$ of the plane containing the great circle. We assume that $\hat{n} \neq (0, 0, 1)$. To find the entries we first work in a coordinate system (x', y', z', w') where the plane $z' = 0$ contains the great circle; this is achieved by a rotation R. Specifically, if

$$\mathbf{R} = \begin{pmatrix} \widehat{(p \times n) \times n}^T & \widehat{p \times n}^T & \hat{n}^T & 0 \\ 0 & 0 & 0 & 1 \end{pmatrix}$$

$$= \begin{pmatrix} \frac{n_x n_z}{\sqrt{1-n_z^2}} & -\frac{n_y}{\sqrt{1-n_z^2}} & n_x & 0 \\ \frac{n_y n_z}{\sqrt{1-n_z^2}} & \frac{n_x}{\sqrt{1-n_z^2}} & n_y & 0 \\ -\sqrt{1-n_z^2} & 0 & n_z & 0 \\ 0 & 0 & 0 & 1 \end{pmatrix},$$

where $p = (0, 0, 1)$ and $\hat{x}$ denotes the normalized vector $x/\|x\|$. We need to find $\mathbf{Q}'$ such that the points where $P'Q'P'^T = 0$ is a cone whose vertex is the point

$$\left(l\sqrt{1-n_z^2}, 0, ln_z\right)$$

and contains the circle

$$\left(\frac{x'}{w'}\right)^2 + \left(\frac{y'}{w'}\right)^2 = 1, \quad z' = 0.$$

First, the coefficients of x' and y' in $x'^2 + y'^2 - 1 = 0$ must equal the coefficients in

$$(x', y', 0, 1)\mathbf{Q}'(x', y', 0, 1)^T = 0.$$

So,

$$\begin{aligned} a = 1, & \quad 2b = 0, & \quad 2d = 0, \\ e = 1, & \quad 2g = 0, & \quad j = -1. \end{aligned}$$

Moreover, the kernel of matrix $\mathbf{Q}'$ is the cone vertex:

$$\mathbf{Q}'\left(l\sqrt{1-n_z^2}, 0, ln_z\right)^T = 0.$$

This fact yields four more constraints:

$$l\sqrt{1-n_z^2} + cln_z = 0$$
$$fln_z = 0$$
$$cl\sqrt{1-n_z^2} + hln_z + i = 0$$
$$iln_z - 1 = 0.$$

Solving for the remaining parameters c, f, h and i we obtain:

$$\mathbf{Q}' = \begin{pmatrix} 1 & 0 & \frac{\sqrt{1-n_z^2}}{n_z} & 0 \\ 0 & 1 & 0 & 0 \\ \frac{\sqrt{1-n_z^2}}{n_z} & 0 & \frac{1-\frac{1}{l^2}-n_z^2}{n_z^2} & \frac{1}{ln_z} \\ 0 & 0 & \frac{1}{ln_z} & -1 \end{pmatrix}.$$

Then

$$\mathbf{Q} = \mathbf{R}\mathbf{Q}'\mathbf{R}^T.$$

We wish to intersect the cone with the plane $z = -m$, so,

$$0 = (x \quad y \quad -m \quad 1) \, \mathbf{R}\mathbf{Q}'\mathbf{R}^T \begin{pmatrix} x \\ y \\ -m \\ 1 \end{pmatrix}$$

$$= (x \quad y \quad 1) \begin{pmatrix} 1 & 0 & 0 & 0 \\ 0 & 1 & 0 & 0 \\ 0 & 0 & -m & 1 \end{pmatrix}$$

$$\times \mathbf{R}\mathbf{Q}'\mathbf{R}^T \begin{pmatrix} 1 & 0 & 0 \\ 0 & 1 & 0 \\ 0 & 0 & -m \\ 0 & 0 & 1 \end{pmatrix} \begin{pmatrix} x \\ y \\ 1 \end{pmatrix}$$

$$= (x \quad y \quad 1) \, \mathbf{C}_{\hat{n}} \begin{pmatrix} x \\ y \\ 1 \end{pmatrix} = 0.$$

We can expand $\mathbf{C}_{\hat{n}}$,

$$\mathbf{C}_{\hat{n}} = \begin{pmatrix} 1 & 0 & 0 & 0 \\ 0 & 1 & 0 & 0 \\ 0 & 0 & -m & 1 \end{pmatrix} \mathbf{R}\mathbf{Q}'\mathbf{R}^T \begin{pmatrix} 1 & 0 & 0 \\ 0 & 1 & 0 \\ 0 & 0 & -m \\ 0 & 0 & 1 \end{pmatrix}$$

$$= \begin{pmatrix} -l^2 n_y^2 n_z^2 - n_x^2(l^2 + n_z^2 - 1) & n_x n_y(l^2 - 1)(n_z^2 - 1) & n_x n_z(l + m)(n_z^2 - 1) \\ n_x n_y(l^2 - 1)(n_z^2 - 1) & -l^2 n_x^2 n_z^2 - n_y^2(l^2 + n_z^2 - 1) & n_y n_z(l + m)(n_z^2 - 1) \\ n_x n_z(l + m)(n_z^2 - 1) & n_y n_z(l + m)(n_z^2 - 1) & -n_z^2(l + m)^2(n_z^2 - 1) \end{pmatrix}$$

The conic $\mathbf{C}_{\hat{n}}$ has the properties

$$f_i = ((l + m)n_x, (l + m)n_y, (-1)^i \sqrt{1 - l^2} - n_z)$$

$$a = \left| \frac{l(l + m)n_z}{l^2 - n_x^2 - n_y^2} \right| \tag{3}$$

$$b = \left| \frac{l + m}{\sqrt{l^2 - n_x^2 - n_y^2}} \right|,$$

where $f_{i=0,1}$ are the foci, a is the minor axis, and b is the major axis; we derive these in the appendix. Notice that the foci are collinear with the image center, and thus the major axis contains the image center.

3.3. Catadioptric Projective Planes

A catadioptric projective plane is the image of the standard projective plane, represented on the sphere, by a central projection from a point on the axis between the north pole and the sphere's center. In the S^2 representation, the points of the standard projective plane are the pairs of antipodal points:

$$\Pi = \{(\pm x, \pm y, \pm z) \mid x^2 + y^2 + z^2 = 1\},$$

and the lines are the set of great circles

$$\Lambda = \left\{ [\pm n_x, \pm n_y, \pm n_z] \mid n_x^2 + n_y^2 + n_z^2 = 1 \right\},$$

where

$$[n_x, n_y, n_z] = \{(x, y, z) \in \Pi \mid xn_x + yn_y + zn_z = 0\},$$

is a single great circle. Therefore $\mathbb{P}^2$ is defined by the pair (Π, Λ). We project from the point on the axis using

the function $s_{l,m}$, obtaining a projective plane $\pi_{l,m} = (s_{l,m}(\Pi), s_{l,m}(\Lambda))$, which we call a *catadioptric projective plane*.

On the sphere all of the axioms necessary for a projective plane are satisfied, as long as antipodal points are identified. The catadioptric projective planes also satisfy these axioms with the understanding that in hyperbolic cases there are two copies of the plane, and that the "points" are always pairs of points, sometimes one pair having points in each of the two copies of the plane, sometimes only in the same copy.

4. Duality

In standard projective geometry there is a one to one correspondence with points and lines of a projective plane. On the sphere, a representation of the projective plane, the correspondence is between a great circle and its poles. We write the dual great circle of a point P as $\tilde{P}$ and the dual point of a great circle ℓ as $\tilde{\ell}$.

An example of their usage is in the following. Suppose we have two points P_1 and P_2 on the sphere and we wish to determine the great circle ℓ between them. We take the dual great circles of the two points, $\tilde{P}_1$ and $\tilde{P}_2$. They must intersect in a pair of points which are antipodal and represented by Q. Taking the dual Q gives the very great circle through the two original points, that is $\ell = \tilde{Q}$. This is because the dual great circle $\tilde{P}$ of any point P on the great circle is a great circle containing the point Q. So intersecting any two yields the point Q.

We call $P_1 \vee P_2$ the great circle between points P_1 and P_2 and $\ell_1 \wedge \ell_2$ the intersection of the great circles ℓ_1 and ℓ_2. We express the fact above in the equations

$$P_1 \vee P_2 = \widetilde{\tilde{P}_1 \wedge \tilde{P}_2},$$

$$\ell_1 \wedge \ell_2 = \widetilde{\tilde{\ell}_1 \vee \tilde{\ell}_2}.$$

The operators $\wedge$ and $\vee$ can be used on the catadioptric projective plane as well, in particular we define for points P_1, P_2 and lines (conics) ℓ_1, ℓ_2 on a catadioptric plane,

$$P_1 \vee P_2 = s_{l,m}\left(s_{l,m}^{-1}(P_1) \vee s_{l,m}^{-1}(P_2)\right)$$

$$\ell_1 \wedge \ell_2 = s_{l,m}\left(s_{l,m}^{-1}(\ell_1) \wedge s_{l,m}^{-1}(\ell_2)\right)$$

Is there such a relationship embedded within the catadioptric projective plane? What properties do the sets of projections of great circles all containing a given point P have? We have seen that the image of a line under catadioptric projection is a conic. We will see that foci of coincident line images lie on a conic which is the projection of the great circle perpendicular to them all; though it is not projected by the same point.

Consider the projection of a point by the map $s_{l,m}$,

$$((l+m)x, (l+m)y, -z + l(-1)^i\sqrt{x^2+y^2+z^2})$$

and the foci of a line image,

$$((l+m)n_x, (l+m)n_y, -n_z + (-1)^i\sqrt{1-l^2}).$$

They look remarkably similar, especially considering that $n_x^2 + n_y^2 + n_z^2 = 1$. Remembering the point-line duality, the foci look like the projection of the dual point of the great circle, i.e. its normal.

Lemma 3. *Let ℓ be a line of a catadioptric projective plane $\pi_{l,m}$ which is the projection of a great circle whose normal is $\hat{n}$. The foci pair of ℓ is the projection of the point $\hat{n}$ by $s_{l',m'}$ where l' and m' satisfy*

$$l + m = l' + m',$$
$$l^2 + l'^2 = 1.$$

Proof: The foci of the line are

$$((l+m)n_x, (l+m)n_y, -n_z + (-1)^i\sqrt{1-l^2}).$$

If

$$l' = \sqrt{1-l^2},$$
$$m' = l + m - \sqrt{1-l^2}$$

then the foci can be rewritten

$$((l'+m')n_x, (l'+m')n_y,$$
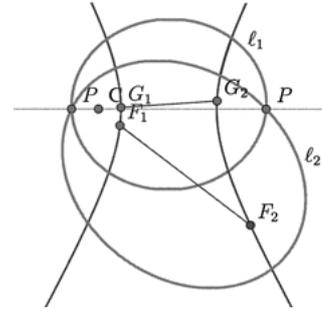$$-n_z + (-1)^i l'\sqrt{n_x^2+n_y^2+n_z^2}).$$

Figure 8. The two ellipses ℓ_1 and ℓ_2 are projections of two lines in space containing the point P. Their foci F_1, F_2, and G_1, G_2 respectively lie on a hyperbola containing the foci of *all* ellipses through P. The foci of this hyperbola are the points in P. The point C is the image center.

This is projection of the point $(n_x, n_y, n_z, 1)$ by $s_{l',m'}$. Conversely, if a point P is projected to a point pair in a catadioptric projective plane $\pi_{l,m}$, this point pair is the foci pair of a line image of a projective plane $\pi_{\sqrt{1-l^2}, l+m-\sqrt{1-l^2}}$. $\square$

Lemma 4. *Let $\{\ell_k\}$ be a set of line images all of which intersect a point P, i.e. for all k, $P \in \ell_k$. Then the locus of foci of the line images lie on a conic c whose foci are the same as the points in P (see Fig. 8).*

Proof: Assume that P is the projection of the point $\hat{n} = (n_x, n_y, n_z)$ on the sphere. Also assume that the lines ℓ_k are images of great circles whose plane's normals are $\hat{m}_k$. Because of rotational symmetry, we may assume without loss of generality that $n_y = 0$. This implies that for some θ_k that

$$\{[\hat{m}_k]\} = \{[-n_z \sin\theta_k, \cos\theta_k, n_x \sin\theta_k]\}.$$

Then the foci of the ℓ_k are,

$$f_i^k = ((l+m)n_z \sin\theta_k, (l+m)\cos\theta_k,$$
$$(-1)^i\sqrt{1-l^2} - n_x \sin\theta_k).$$

But these are the pair of points in the projection of $\hat{m}_k$ by

$$s_{\sqrt{1-l^2}, l+m-\sqrt{1-l^2}}.$$

Therefore this point is in the image of the line $\hat{n}$ by this same projection. Its foci are

$$f_i = ((l+m)n_x, 0, (-1)^i l - n_z),$$

which is the projection of $\hat{n}$ by $s_{l,m}$. $\square$

We use Lemmas 3 and 4 to prove the following duality theorem.

Theorem 2 (*Duality*). *If* $\pi_{l,m} = (\Pi_1, \Lambda_1)$ *and* $\pi_{l',m'} = (\Pi_2, \Lambda_2)$ *are two catadioptric planes such that*

$$l^2 + l'^2 = 1 \quad and \quad l + m = l' + m',$$

then $f_{l,m}$, *which gives the foci of a line image in the context of some catadioptric plane* $\pi_{l,m}$, *maps as follows*,

$$f_{l,m} : \Lambda_1 \rightarrow \Pi_2,$$
$$f_{l',m'} : \Lambda_2 \rightarrow \Pi_1,$$

and their inverse mappings exist. In addition, incidence relationships are preserved by $f_{l,m}$:

$$P_1 \vee P_2 = f_{l,m}^{-1}\left(f_{l',m'}^{-1}(P_1) \wedge f_{l',m'}^{-1}(P_2)\right),$$
$$\ell_1 \wedge \ell_2 = f_{l,m}(f_{l',m'}(\ell_1) \vee f_{l',m'}(\ell_2)),$$

where $P_1, P_2 \in \Pi_1$ *and* $\ell_1, \ell_2 \in \Lambda_2$.
   We call the projective planes, $\pi_{l,m}$ *and* $\pi_{l',m'}$, *dual catadioptric projective planes.*

Proof: We have already shown the first part of the theorem in Lemma 3. It only remains to show that incidence relationships are preserved. This follows from Lemma 4 and the fact that incidence relationships are already known to be preserved on the sphere by the mapping taking antipodal points to great circles and vice versa.   □

Corollaries.

1. *Perspective projection* ($l = 0$) *is dual to parabolic projection* ($l' = 1$). *This means that the parabolic projection of a line is a circle whose center* (*the foci collapse to a single point*) *is the perspective projection of the normal of the plane containing the line. It also implies that the parabolic projection of a pair of antipodal points are two points whose perpendicular bisector is the projection of the great circle dual to the antipodal point pair.*
2. *A catadioptric projection with a mirror of eccentricity* ϵ *is dual to a catadioptric projection with mirror eccentricities* $|\frac{1-\epsilon}{1+\epsilon}|$ *and* $|\frac{1+\epsilon}{1-\epsilon}|$ (*one is a hyperbolic projection; the other is an equivalent elliptic projection*).
3. *A catadioptric projection with eccentricity* $\pm 1 + \sqrt{2}$ *is self-dual* ($l = \frac{1}{\sqrt{2}}$). *In this case the foci of a*

projected great circle are exactly the projections of the dual points.

5.   Practical Implications: Calibration

The presented unifying theory of catadioptric projections enables a direct and natural insight into the invariances of these projections. The perspective projection is a degenerate case of a catadioptric projection, in the sense that antipodal points on the sphere are projected to single points, whereas in the parabolic and hyperbolic cases antipodal points are projected to two different points. In this section, we show that it is possible to calibrate a catadioptric sensor with as few as two lines.

If we assume that CCD-mount and lens do not induce radial distortion and satisfy the pin-hole model (for a hyperbolic configuration) or the orthographic model (for a parabolic system), then the intrinsic parameters of a general catadioptric projection are the eccentricity of the mirror, the combined focal length of the mirror and camera, the image center, and any skew and aspect ratio induced by the sensor. It is the task of calibration to estimate these parameters. We examine the possibility or impossibility of calibrating from lines in a single frame. We have previously demonstrated a calibration algorithm for the parabolic case (Geyer and Daniilidis, 1999) whose input is at least two sets of parallel lines. At the end of this section we show a more general (arbitrary sets of lines) and simplified algorithm.

First, let us gain some intuition into why it is possible to calibrate non-perspective catadioptric sensors from lines. We examine the perspective case first. Assuming that aspect ratio is one and skew is zero, there are three intrinsic parameters, namely the image center and focal length. The image of a line in space is a line in the image plane, and any given line may be uniquely determined by two points. From any image line it is possible only to determine the orientation of the plane containing the line in space and the focal point; the orientation of this plane can be parameterized by two parameters. Given n lines, how many constraints are there and how many unknowns? If for some n the number of constraints exceeds the number of unknowns, then we have a hope of obtaining the unknowns, and thus calibrate the sensor. However, for every line added we gain two more constraints and two more unknowns; we are always short by three equations. Therefore self-calibration *from lines*, without any metric information, and in one frame is not possible in the perspective case.

What about the parabolic case? There are a total of three unknowns, focal length and image center (alone giving two unknowns). The projection of any line is a circle, and which is completely specified by as few as three points, therefore three constraints. The orientation of the plane containing the line gives two unknowns. So, for every line that we obtain we reduce the number of unknowns by one. If there are three lines, we have 9 constraints and 9 unknowns, and thus we can perform self-calibration with only three lines.

Finally the hyperbolic case. There are four unknowns (eccentricity, focal length and image center) and each line adds two for orientation. The projection of a line is a conic which may be specified by five points. Thus when we have two lines we have 8 unknowns and 10 constraints. So, with only two lines the system is over-determined, but nevertheless we can still perform a calibration.

We give here a simple and compact algorithm for calibrating the parabolic projection. It is based on the fact that a sphere, whose equator is a circle in the image plane, contains the point $(c_x, c_y, 2f)$, where $(c_x, c_y, 0)$ is assumed to be the image center, though initially unknown. This is by symmetry, since the image circle intersects the fronto-parallel plane at points a distance $2f$ from the image center. Thus the intersection of at least three spheres so-constructed produces the points $(c_x, c_y, \pm 2f)$, giving us both image center and focal length simultaneously (see Fig. 9).

In the presence of noise, the intersection is not defined for more than three spheres, yet we may minimize the distance from a point to all of the spheres, i.e. find the point (c_x, c_y, f) such that

$$\sum_{i=1}^{n} \left((d_x^i - c_x)^2 + (d_y^i - c_y)^2 + 4f^2 - r_i^2 \right)^2 \quad (4)$$

is a minimum over all points. Here (d_x^i, d_y^i) is the center of the i-th image circle, and r_i is its radius. The intersection is not defined for fewer than three spheres, since the intersection of two spheres gives only the circle within which the point lies, but not the point itself.

In the parabolic case it is also possible to calibrate the skew and aspect ratio. Non-unit aspect ratio and skew transform a parabolic image so that the images of lines are ellipses with the same aspect ratio. There is a single linear transformation, *modulo scale*, which transforms this distorted image to one in which line images are again circles. To find this unique transformation, we minimize over the quotient space of possible representative transformations the residuals of circles fitted to transformed points which are known to lie on line images.

We next describe an experiment (see Fig. 10) in which we have taken an image of a small $8\frac{1}{2}'' \times 11''$ calibration target with a folded catadioptric camera. We fit circles to the grid points and perform a calibration. Then we estimate the normal of the plane containing the
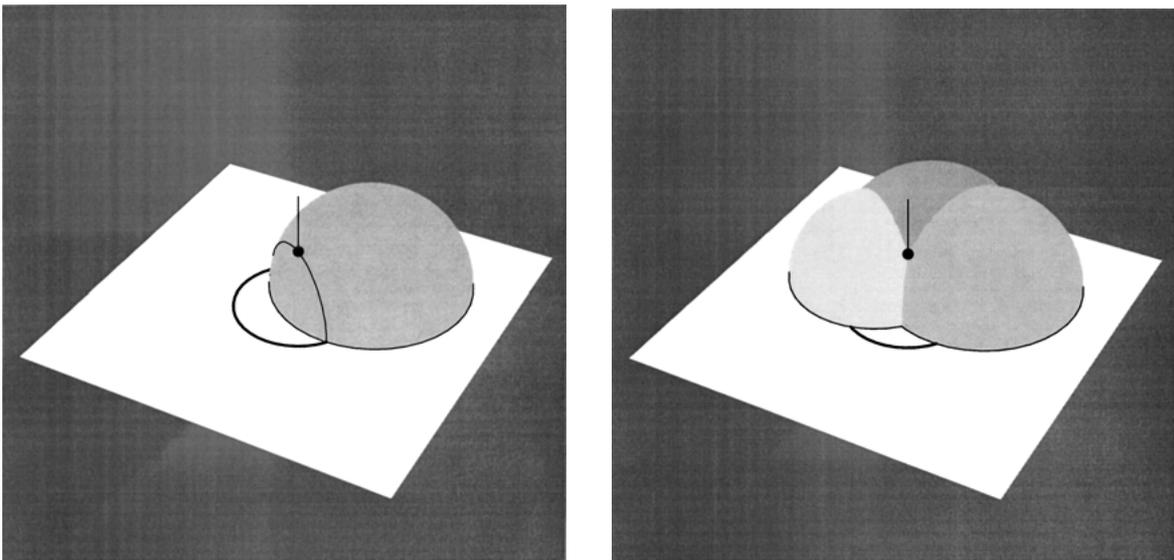

Figure 9. Left: Sphere whose equator is a line image which contains the point $(c_x, c_y, 2f)$. The circle in the image plane is the fronto-parallel horizon. Right: Intersection of three such spheres to determine this point.
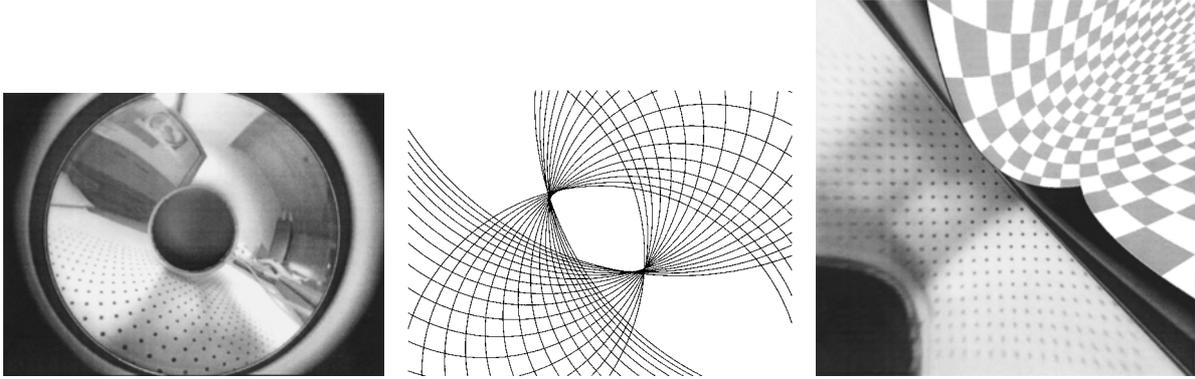
Figure 10.   Left: Original image taken by a folded catadioptric camera. Middle: Circles fitted to points captured from the grid. Notice that the lines of the grid are parallel and thus their projections, circles, intersect in the image at vanishing points. Using these line images we perform a calibration and rectification, i.e. finding the normal of the plane containing the grid. Right: A reprojection to a plane parallel to the grid.

grid and then project to a plane parallel to the plane of the grid, i.e. a rectification. Rectification is described in Geyer and Daniilidis (1999) and can be achieved with only affine knowledge. Given two sets of parallel lines their two double vanishing points define a circle on the catadioptric image. The center of this circle is the projection of the normal of the plane spanned by the two directions up to the known focal length. In the rectification, we see that to a good approximation lines have been mapped to lines, and also that angles are preserved.

6.   Conclusion

In this paper, we presented a novel theory on the geometry of central catadioptric systems. We proved that every such projection can be modeled with the projection of the sphere to a horizontal plane from a point on the vertical axis of the sphere. Hence, any catadioptric projection is equivalent to a central projection of the spherical representation of the projective plane. Using this equivalence we observe that images of lines in space are mapped to great circles on the sphere and to conic sections on the catadioptric image plane. We show that each mirror shape has its dual and that dual projections map poles of great circles on the sphere to

the foci of the conic sections corresponding to the great circles of the poles.

The first practical implication concerns the determination of the image center, the effective focal length, and the mirror eccentricity from a single view of line images. The perspective case proves to be the only one not providing the sufficient constraints for such a calibration.

Our ongoing work addresses multiple uncalibrated catadioptric views with possibly varying camera parameters. We mention here the parabolic case as an example. We proved in this paper the equivalence of the parabolic case to the projection on the sphere followed by a stereographic projection. Stereographic projection is a conformal mapping: the angle between two great circles on the sphere is equal to the angle between their images. We are going to analyze such constraints in multiple views and give the sufficient conditions on translation directions and rotation axes for the recovery of camera parameters, motion, and structure.

Appendix 1

We would like to derive the properties of the conic whose quadratic form is,

$$\mathbf{C}_{\hat{n}} = \begin{pmatrix} -l^2 n_y^2 n_z^2 - n_x^2(l^2 + n_z^2 - 1) & n_x n_y(l^2 - 1)(n_z^2 - 1) & n_x n_z(l + m)(n_z^2 - 1) \\ n_x n_y(l^2 - 1)(n_z^2 - 1) & -l^2 n_x^2 n_z^2 - n_y^2(l^2 + n_z^2 - 1) & n_y n_z(l + m)(n_z^2 - 1) \\ n_x n_z(l + m)(n_z^2 - 1) & n_y n_z(l + m)(n_z^2 - 1) & -n_z^2(l + m)^2(n_z^2 - 1) \end{pmatrix}.$$

We wish to put the conic into a normal form in which we can obtain the major and minor axes as well as the location of the foci. First we apply the rotation matrix

$$\mathbf{R} = \begin{pmatrix} \frac{n_x}{\sqrt{n_x^2+n_y^2}} & \frac{n_y}{\sqrt{n_x^2+n_y^2}} & 0 \\ -\frac{n_y}{\sqrt{n_x^2+n_y^2}} & \frac{n_x}{\sqrt{n_x^2+n_y^2}} & 0 \\ 0 & 0 & 1 \end{pmatrix},$$

obtaining

$$\mathbf{RC}_{\hat{n}}\mathbf{R}^T = \begin{pmatrix} -(n_x^2+n_y^2)(l^2+n_z^2-1) & 0 & (l+m)\sqrt{n_x^2+n_y^2}n_z(n_z^2-1) \\ 0 & -l^2(n_x^2+n_y^2)n_z^2 & 0 \\ (l+m)\sqrt{n_x^2+n_y^2}n_z(n_z^2-1) & 0 & -(l+m)^2n_z^2(n_z^2-1) \end{pmatrix}.$$

Application of the matrix

$$\mathbf{T} = \begin{pmatrix} 1 & 0 & 0 \\ 0 & 1 & 0 \\ \frac{(l+m)n_z(n_z^2-1)}{\sqrt{n_x^2+n_y^2}(l^2+n_z^2-1)} & 0 & 1 \end{pmatrix},$$

centers the conic at the origin, and we have

$$\mathbf{TRC}_{\hat{n}}\mathbf{R}^T\mathbf{T}^T = \begin{pmatrix} -(n_x^2+n_y^2)(l^2+n_z^2-1) & 0 & 0 \\ 0 & -l^2(n_x^2+n_y^2)n_z^2 & 0 \\ 0 & 0 & -\frac{l^2(l+m)^2n_x^2(n_z^2-1)}{l^2+n_z^2-1} \end{pmatrix}.$$

Normalizing and substituting $n_z^2 = 1 - n_x^2 - n_y^2$, we have

$$\mathbf{C}' = \begin{pmatrix} \frac{(-l^2+n_x^2+n_y^2)^2}{l^2(l+m)^2n_z^2} & 0 & 0 \\ 0 & -\frac{-l^2+n_x^2+n_y}{(l+m)^2} & 0 \\ 0 & 0 & -1 \end{pmatrix}.$$

Thus the major axis

$$a = \left| \frac{l(l+m)n_z}{-l^2+n_x+n_y^2} \right|,$$

and minor axis

$$b = \left| \frac{l+m}{\sqrt{-l^2+n_x^2+n_y^2}} \right|.$$

Now to find the foci. An ellipse with quadratic form

$$\begin{pmatrix} a^{-2} & 0 & 0 \\ 0 & b^{-2} & 0 \\ 0 & 0 & -1 \end{pmatrix},$$

has eccentricity $\sqrt{1 - \frac{b^2}{a^2}}$ and foci at $(\pm a\epsilon, 0, 1)$. A hyperbola with quadratic form

$$\begin{pmatrix} a^{-2} & 0 & 0 \\ 0 & -b^{-2} & 0 \\ 0 & 0 & -1 \end{pmatrix},$$

has eccentricity $\sqrt{1 + \frac{b^2}{a^2}}$ and foci at $(\pm a\epsilon, 0, 1)$. Therefore a conic with quadratic form

$$\begin{pmatrix} \alpha & 0 & 0 \\ 0 & \beta & 0 \\ 0 & 0 & -1 \end{pmatrix}$$

has foci at $(\sqrt{\alpha^{-1} - \beta^{-1}}, 0, 1)$. Hence, the foci of $\mathbf{C}'$ are

$$\left(\pm \frac{\sqrt{1-l^2}(l+m)\sqrt{n_x^2+n_y^2}}{-l^2+n_x^2+n_y^2}, 0, 1 \right).$$

Now translate and rotate back to the original coordinate system and we find that the foci of $\mathbf{C}_{\hat{n}}$ are

$$f_i = \left(\frac{(l+m)n_x((-1)^i\sqrt{1-l^2} - n_z)}{-l^2 + n_x^2 + n_y^2}, \right.$$

$$\left. \frac{(l+m)n_y((-1)^i\sqrt{1-l^2} - n_z)}{-l^2 + n_x^2 + n_y^2}, 1 \right)$$

$$= \left((l+m)n_x, (l+m)n_y, (-1)^i\sqrt{1-l^2} - n_z \right).$$

Note

1. We do not consider the case where ℓ is not perpendicular to F_1F_2; in such a case, the projection differs from the one defined above only by a line homography (or by a plane homography in the three dimensional extension).

References

Baker, S. and Nayar, S. 1988. A theory of catadioptric image formation. In *Proc. Int. Conf. on Computer Vision*, Bombay, India, Jan. 3–5, 1998, pp. 35–42.

Baker, S. and Nayar, S. 1999. A theory of single-viewpoint catadioptric image formation. *International Journal of Computer Vision*, 35:175–196.

Benosman, R., Deforas, E., and Devars, J. 2000. A new catadioptric sensor for panoramic vision of mobile robots. In *IEEE Workshop on Omnidirectional Vision*, Hilton Head, SC, June 12, 2000, pp. 112–118.

Benosman, R. and Kang, S. 2000. *Panoramic Vision*. Springer-Verlag: New York, Berlin, Heidelberg.

Bogner, S. 1995. An introduction to panospheric imaging. In *Proc. IEEE Conf. Systems, Man, and Cybernetics*, Vancouver, BC, pp. 3099–3116.

Boult, T. 1998. Remote reality demonstration. In *IEEE Conf. Computer Vision and Pattern Recognition*, Santa Barbara, CA, June 23–25, 1998, pp. 966–967.

Bruckstein, A. and Richardson, T. 2000. Omniview cameras with curved surface mirrors. In *IEEE Workshop on Omnidirectional Vision*, Hilton Head, SC, June 12, 2000, originally published as Bell Labs Technical Memo, 1996, pp. 79–86.

Chahl, J. and Srinivasan, M. 1997. Reflective surfaces for panoramic imaging. *Applied Optics*, 36:8275–8285.

Daniilidis, K. (Ed.). 2000. *IEEE Workshop on Omnidirectional Vision*, Hilton Head Island, SC, June 12, 2000.

Geyer, C. and Daniilidis, K. 1999. Catadioptric camera calibration. In *Proc. Int. Conf. on Computer Vision*, Kerkyra, Greece, Sept. 20–23, 1999, pp. 398–404.

Greguss, P. 1985. The tube-peeper: A new concept in endoscopy *Optics and Laser Technology*, 32:41–45.

Hartley, R. 2000. Chirality. *International Journal of Computer Vision*, 26:41–61.

Hecht, E. and Zajac, A. 1997. *Optics* (3rd edn.). Addison-Wesley: Reading, MA.

Hicks, R. and Bajcsy, R. 2000. Catadioptric sensors that approximate wide-angle perspective projections. In *IEEE Conf. Computer Vision and Pattern Recognition*, Hilton Head Island, SC, June 13–15, 2000, pp. 545–551.

Hong, J., Tan, X., Weiss, R., and Riseman, E. 1991. Image-based homing. In *IEEE Int. Conf. Robotics and Automation*, pp. 620–625.

Kang, S. 2000. Catadioptric self-calibration. In *IEEE Conf. Computer Vision and Pattern Recognition*, Hilton Head Island, SC, June 13–15, 2000, pp. I–201–207.

Land, M. 1981. Optics and vision. in inverterbrates. In *Handbook of Sensory Physiology*, Autrum, H. (Ed.). Vol. VII/6B, Springer Verlag: Berlin, ch. 4, pp. 472–585.

Laveau, S. and Faugeras, O. 1996. Oriented projective geometry in computer vision. In *Proc. Fourth European Conference on Computer Vision*, Cambridge, UK, April 14–18, 1996, B. Buxton (Ed.). Springer: Berlin, pp. 147–156. LNCS, 1064.

Leonardis, A. and Jogan, M. 2000. Robust localization using eigenspace of spinning-images. In *IEEE Workshop on Omnidirectional Vision*, Hilton Head, SC, June 12, 2000, pp. 37–46.

Majumder, A., Gopi, M., Seales, B., and Fuchs, H. 1999. Immersive teleconferencing: A new algorithm to generate seamless panoramic video imagery. In *Proceedings of the Seventh ACM International Conference on Multimedia*, pp. 169–178.

Nalwa, V. 1996. A true omnidirectional viewer. Technical report, Bell Labs, Holmdel, NJ.

Nayar, S. 1997. Catadioptric omnidirectional camera. In *IEEE Conf. Computer Vision and Pattern Recognition*, Puerto Rico, June 17–19, 1997, pp. 482–488.

Nayar, S. and Peri, V. 1999. Folded catadioptric cameras. In *IEEE Conf. Computer Vision and Pattern Recognition*, Fort Collins, CO, June 23–25, 1999, pp. 217–225.

Needham, T. 1997. *Visual Complex Analysis*. Clarendon Press: Oxford.

Nene, S. and Nayar, S. 1998. Stereo with mirrors. In *Proc. Int. Conf. on Computer Vision*, Bombay, India, Jan. 3–5, 1998, pp. 1087–1094.

Onoe, Y., Yamazawa, K., Takemura, H., and Yokoya, N. 1998. Telepresence by real-time view-dependent image generation from omnidirectional video streams. *Computer Vision and Image Understanding*, 71:588–592.

Pajdla, T., Werner, T., and Hlavac, V. 1998. Oriented projective reconstruction. In *Proc. Austrian Association for Pattern Recognition*.

Penrose, R. and Rindler, W. (Eds). 1984. *Spinors and Space-Time*. Cambridge University Press: Cambridge, UK.

Rees, D.W. 1971. Panoramic television viewing system. United States Patent No. 3, 505, 465, April 1970.

Shah, S. and Aggarwal, J. 1996. Intrinsic parameter calibration procedure for a (high-distortion) fish-eye lens camera with distortion model and accuracy estimation. *Pattern Recognition*, 29:1775–1788.

Shum, H.-Y. and Szeliski, R. 2000. Systems and experiment paper: Construction of panoramic image mosaics with global and local alignment. *International Journal of Computer Vision*, 36:101–130.

Stolfi, J. 1991. *Oriented Projective Geometry*. Academic Press: Boston.

Sturm, P. 2000. A method for 3D-reconstruction of piecewise planar objects from single panoramic images. In *IEEE Workshop on Omnidirectional Vision*, Hilton Head, SC, June 12, 2000, pp. 119–126.

Svoboda, T., Pajdla, T., and Hlavac, V. 1998. Epipolar geometry for panoramic cameras. In *Proc. 5th European Conference on Computer Vision*, pp. 218–231.

Swaminathan, R. and Nayar, S. 2000. Non-metric calibration of wide-angle lenses and polycameras. In *IEEE Conf. Computer Vision and Pattern Recognition*, Hilton Head Island, SC, June 13–15, 2000, pp. II–413–419.

Taylor, C. 2000. Video plus. In *IEEE Workshop on Omnidirectional Vision*, Hilton Head, SC, June 12, 2000, pp. 3–10.

Toomer, G. 1976. *Diocles On Burning Mirrors*. Sources in the History of Mathematics and the Physical Sciences. Springer-Verlag: Berlin.

Winters, N., Gaspar, J., Lacey, G., and Santos-Victor, J. 2000. Omnidirectional vision for navigation In *IEEE Workshop on Omnidirectional Vision*, Hilton Head, SC, June 12, 2000, pp. 21–28.

Yagi, Y. 1999. Omnidirectional sensing and its application. *IEICE Trans. Inform. and Systems*, 3:568–579.

Yagi, Y., Kawato, S., and Tsuji, S. 1994. Real-time omnidirectional image sensor (COPIS) for vision-guided navigation. *Trans. on Robotics and Automation*, 10:11–22.

Zheng, J. and Tsuji, S. 1992. Panoramic representation for route recognition by a mobile robot. *International Journal of Computer Vision*, 9:55–76.

Zhu, Z., Rajasekar, K., Riseman, E., and Hanson, A. 2000. Panoramic virtual stereo vision of cooperative mobile robots for localizing 3D moving objects. In *IEEE Workshop on Omnidirectional Vision*, Hilton Head, SC, June 12, 2000, pp. 29–36.